Anatomical Connectivity of the Visuospatial Attentional Network in Schizophrenia: A Diffusion Tensor Imaging Tractography Study

Elise Leroux, Ph.D., Nicolas Poirel, Ph.D., Sonia Dollfus, M.D., Ph.D.

Objective: In healthy individuals, the visuospatial attentional network consists of frontoparietal bundles; however, the anatomical organization of this network in persons with schizophrenia remains largely unknown. Using diffusion tensor imaging–based tractography, the authors investigated the white matter integrity and volume of frontoparietal and frontotemporo-occipital bundles in the right and left hemispheres and studied their structural asymmetry in persons with schizophrenia and in healthy individuals.

Methods: This study included 34 participants with schizophrenia and 69 healthy individuals. Integrity parameters and volume were calculated in the three branches of the superior longitudinal fasciculus (SLF I, II, and III), the inferior longitudinal fasciculus, and the inferior fronto-occipital fasciculus in both hemispheres.

Results: In the SLF II and SLF III of the right hemisphere, healthy individuals showed greater integrity, compared with participants with schizophrenia. Both groups presented increased integrity in the SLF III of the right hemisphere, compared with the SLF III of the left hemisphere, but only healthy individuals had this pattern regarding the SLF II. Bundle volumes did not differ between groups.

Conclusions: This study is the first to describe the structural hemispheric lateralization and organization of the visuospatial attentional network in persons with schizophrenia. The main findings indicate loss of integrity in the SLF II, associated with loss of asymmetry in participants with schizophrenia, compared with healthy individuals, suggesting a potential substrate of attentional deficits.

J Neuropsychiatry Clin Neurosci 2020; 32:266–273;
doi: 10.1176/appi.neuropsych.19040101

Anatomical connectivity studies in healthy individuals and in persons with visuospatial attention–spatial neglect have demonstrated that the superior longitudinal fasciculus (SLF), inferior fronto-occipital fasciculus (IFOF), and inferior longitudinal fasciculus (ILF) are strongly linked to visuospatial attentional abilities (1, 2). Right-handed healthy individuals present a left-hemispheric dominance for language (3–5) and a right-hemispheric dominance for visuospatial attention (1, 2). In contrast, persons with schizophrenia present decreased leftward hemispheric functional lateralization for language (6, 7) and underlying anatomical organization of disrupted white matter (8–12). No previous studies have investigated the anatomy or structural asymmetry of the SLF, IFOF, and ILF in schizophrenia, despite anatomically related visual attentional impairments (13–15) that may contribute to problems with everyday function. Accordingly, identifying anatomical abnormalities underlying these attentional deficits in persons with schizophrenia is important.

The visuospatial attentional network consists of several cortical epicenters that form a large-scale and bilaterally distributed neurocognitive system (16), interconnected by fiber bundles. Corbetta and Shulman (17) proposed a subdivision of these epicenters into dorsal and ventral streams in healthy individuals. The SLF commonly supports the dorsal and ventral streams and is subdivided into the dorsal (SLF I), middle (SLF II), and ventral (SLF III) branches (18). SLF II mediates direct communication between SLF III and SLF I. Globally, these streams are involved in various visuospatial attentional abilities (2, 19, 20). Thiebaut de Schotten et al. (2) found a lateralized dorsal-ventral gradient with a symmetric SLF I between the two hemispheres, a rightward asymmetry of the SLF III, and a tendency to a larger SLF II in the right hemisphere. Another group has replicated the rightward asymmetry of the SLF III (21). Thiebaut de Schotten et al. (2) demonstrated that asymmetry of the SLF II could predict behavioral performance on a visuospatial attention task, showing that a larger

Online supplemental materials can be found by selecting "View Options" (located above the Abstract when accessing article on computer or tablet) or "About" (located above the title when accessing on smartphone).

right-hemisphere SFL II corresponds with faster reaction times in the left hemifield during a line bisection task.

Other fiber bundles, such as the IFOF and ILF, also contribute to the ventral processing stream. These bundles also are involved in various visuospatial attentional abilities (1, 22–25). Regarding their anatomical asymmetry, Chechlacz et al. (21) found that IFOF volume in healthy individuals is distributed symmetrically between the two hemispheres and that the IFOF is lateralized rightward with respect to integrity. In their work, the data were extracted to diffusion tensor imaging (DTI), which characterizes properties of white matter (26). Recent studies have identified leftward anatomical asymmetry for the ILF with respect to integrity (27, 28).

Using DTI tractography, we performed the first assessment of the integrity and volume of fasciculi underlying the visuospatial attentional network (SLF I, SLF II, SLF III, ILF, and IFOF) in both hemispheres and studied their structural asymmetry in persons with schizophrenia and in healthy individuals. Our hypothesis was that compared with healthy individuals, persons with schizophrenia would show a loss of white matter pathway integrity and of structural asymmetry.

METHODS

All participants provided informed, written consent in accordance with the Declaration of Helsinki, and the local ethics committee (Comité de Protection des Personnes Nord-Ouest, France) approved the experimental protocol.

Participants

Participants were recruited from Caen University Hospital (Caen, France) and the surrounding community. Participants with schizophrenia or schizoaffective disorder were identified by using DSM-IV criteria and were assessed with the Positive and Negative Syndrome Scale (PANSS) (29). The healthy individuals did not meet criteria for lifetime psychotic disorders (they did not take antipsychotic-anxiolytic medication) or substance dependence (including alcohol), as assessed by the Mini International Neuropsychiatric Interview. Lifetime habits, such as tobacco consumption, were not collected for either group, although this variable could be an additional confounding factor in the interpretation of our findings. All participants were required to be free of neurological disorders and cerebral abnormalities.

Data Acquisition

Neuroimaging data were acquired on a 3-T scanner (Intera Achieva, Philips Medical Systems, Eindhoven, the Netherlands). Three-dimensional, high-resolution T_1-weighted brain volumes were acquired (three-dimensional fast-field echo turbo-field echo sequence: 256 × 256 matrix size with 180 contiguous slices, 256-mm field of view, 1-mm isotropic resolution, sagittal slice orientation, 20-ms repetition time, 4.6-ms echo time, 10° flip angle, 800-ms inversion time, and a SENSE factor of 2). In addition, a T_2-weighted scan was acquired for each participant (T_2 turbo spin echo sequence: 256 × 256 matrix size with 81 contiguous slices, 256-mm field of view, 2-mm isotropic resolution, sagittal slice orientation, 5,500-ms repetition time, 80-ms echo time, 90° flip angle, and a SENSE factor of 2).

We obtained diffusion-weighted images by using a diffusion-weighted imaging sequence from 21 directions with one image without diffusion weighting (factor b=1,000 seconds/mm^2, 112 × 112 matrix size with 70 contiguous slices, 224-mm field of view, 2-mm isotropic resolution, axial slice orientation, 8,500-ms repetition time, 81-ms echo time, 90° flip angle, and a SENSE factor of 2.5).

Data Analysis

For preprocessing of anatomical data, we used SPM5 software subroutines (Statistical Parametric Mapping, Wellcome Department of Cognitive Neurology, London, http://www.fil.ion.ucl.ac.uk/spm), which allowed us to obtain classical anatomical images in MNI space (Montreal Neurological Institute, Canada). We chose normalization parameters by default and used the deformation field from the normalization for subsequent processing of DTI data.

The method used to extract diffusion values into the different tracts has been published previously (8, 30). Briefly, the preprocessing of diffusion data used different steps (movement and eddy current correction; calculation of diffusion tensor model [DTIFIT; FDT FMRIB's Diffusion Toolbox]) of FSL software (FLIRT, FMRIB Software Library, Oxford, United Kingdom, http://www.fmrib.ox.ac.uk/fsl), which allowed us to obtain diffusion maps of fractional anisotropy (FA), radial diffusivity (RD), and mean diffusivity (MD) (RD and MD in mm^2/second) for each participant. Fiber tracking was reconstructed from the diffusion-weighted images for each participant within the frontoparietal network in both the right and left hemispheres. Thus the SLF was subdivided into three branches: $SLFI_R$/$SLFI_L$, $SLFII_R$/$SLFII_L$, and $SLFIII_R$/$SLFIII_L$ (R, right; L, left). The $IFOF_R$/$IFOF_L$ and the ILF_R/ILF_L were also reconstructed. To reconstruct all of these fasciculi in each participant, we applied a probabilistic tractography method to transfer regions used as "seed" or "avoid" regions (belonging to automated anatomical labeling gray matter [31] or Mori's gray matter and white matter atlases [32]) into the diffusion space where the different tracts were created (33, 34).

The $SLFI_R$/$SLFI_L$ was reconstructed between the left or right superior frontal and superior parietal gyri, respectively; the SLF II between the middle frontal and inferior parietal gyri (angular gyrus); and the SLF III between the inferior frontal and inferior parietal gyri (2, 35), according to Mori's gray matter atlas (Figure 1). We used the temporal lobe as the "avoid" region to exclude fibers of the arcuate fasciculus. The $IFOF_R$/$IFOF_L$ was reconstructed between the inferior frontal and middle occipital gyri (25, 36), according to Mori's gray matter atlas, and we used the ILF from Mori's white matter atlas as the "avoid" region because of fibers in common with IFOF. Then, we reconstructed the ILF_R/ILF_L between the anterior temporal pole (automated anatomical labeling gray matter atlas) and inferior occipital cortex (Mori's gray matter atlas) (36, 37) and used the IFOF as the "avoid" region (Mori's white matter atlas).

FIGURE 1. Regions of interest in the probabilistic tractography[a]

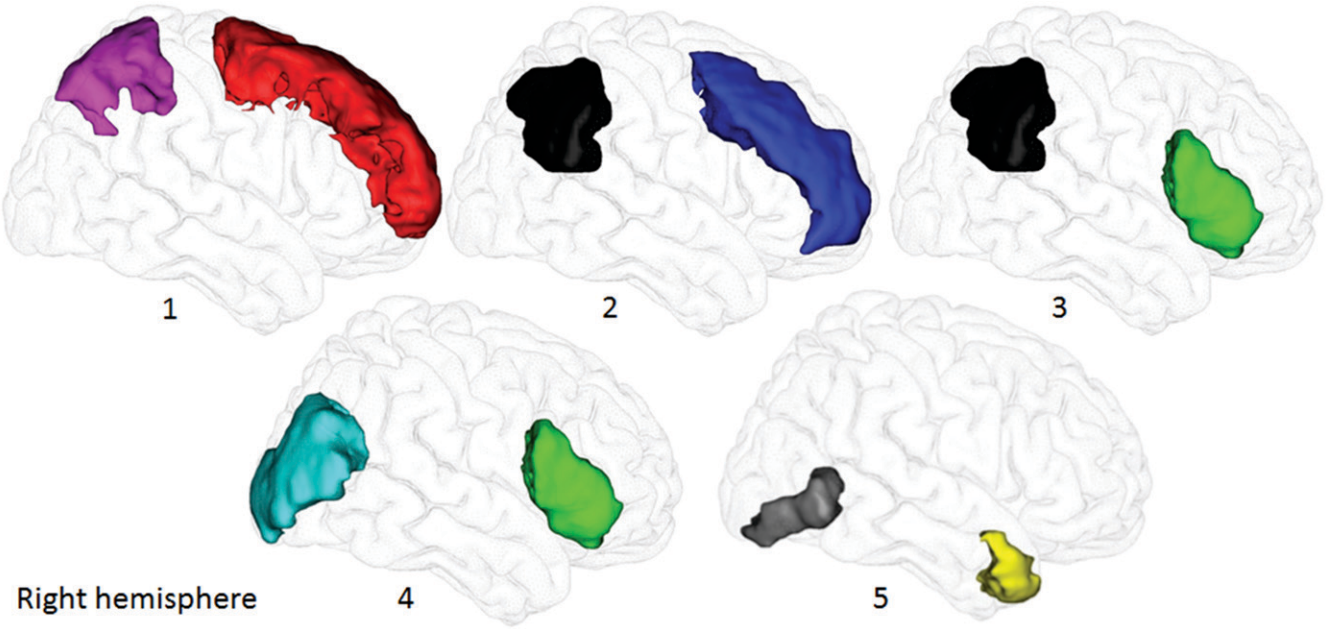

[a] The superior frontal (red) and superior parietal (purple) gyri were used to reconstruct branch I of the superior longitudinal fasciculus (SLF) (image 1). The middle frontal (navy blue) and inferior parietal (black) gyri were used to reconstruct SLF II (image 2). The inferior frontal (green) and inferior parietal gyri (black) were used to reconstruct SLF III (image 3). The inferior frontal and middle occipital (light blue) gyri were used to reconstruct the inferior fronto-occipital fasciculus (image 4). The inferior occipital gyrus (gray) and the anterior temporal pole (yellow) were used to reconstruct the inferior longitudinal fasciculus (image 5). All regions in the diffusion space are based on Mori's gray matter atlas (32), except the anterior temporal pole, which is based on the automated anatomical labeling gray matter atlas (31). These regions are shown in the right hemisphere; however, the same regions were used in reconstruction of five tracts in the left hemisphere.

Next, we registered the ten tracts and diffusion maps for each participant in the MNI space. For this purpose, we used a deformation field previously calculated by using a fully automated in-house normalization method to individually extract and compare mean values for all diffusion parameters (anisotropy values: FA; diffusivity values: RD and MD) and white matter volume (number of voxels) between groups. In brief, this method consists of initially registering rigidly the native T_2-weighted volume onto the T_1 acquisition, followed by rigid and nonlinearly spatially normalized registration of the individual image without diffusion weighting onto the first-created image. The transformation matrix, resulting from this spatial registration, is combined with the transferred individual T_1-weighted images in the MNI space in order to register individual tracts/diffusion maps directly into standard space (30). Per standard practice, we defined white matter abnormalities as loss of integrity characterized by decreased FA (axonal degeneration) and increased RD/MD (demyelination) (26, 30, 38). (All individual fasciculi in the diffusion space in participants with schizophrenia are displayed in Figure S1 in the online supplement.)

Statistical Analysis

Analyses of covariance (ANCOVAs) were computed separately to test differences in the integrity of diffusion data between the two groups and between the two hemispheres for each tract. For each tract (SLF I, SLF II, SLF III, IFOF, and ILF), we performed a repeated-measures ANCOVA (with participants as random effect) with each diffusion parameter (FA, RD, and MD) as the dependent variable and group and hemisphere as independent factors. The analyses included sex and tract volume as covariates, and the group-by-hemisphere interaction was tested. Using Tukey's HSD test to correct for multiple comparisons, we conducted post hoc analyses when a significant main effect emerged.

Intragroup correlation analyses (Pearson) between anatomical and clinical data were also conducted for participants with schizophrenia to evaluate the impact of antipsychotic dosages (in chlorpromazine equivalents), duration of illness, and severity of symptoms (PANSS positive, negative, and general subscores and total PANSS scores) on white matter integrity/volume and their asymmetry index (AI). AI was based on the following formula: AI=100 × (right hemisphere – left hemisphere) / (right hemisphere + left hemisphere), where positive (AI $>$ 0) and negative (AI $<$ 0) AIs correspond to rightward and leftward asymmetries, respectively. With a Bonferroni correction for multiple comparisons, correlations were considered statistically significant when $p<0.0071$.

We performed all statistical analyses with JMP v13.0 Software (SAS Institute, Cary, N.C.). The significance level for other analyses was set at $p<0.05$.

RESULTS

Thirty-four participants with schizophrenia or schizoaffective disorder and 69 unaffected individuals met study inclusion criteria. All participants were right-handed (self-

reported). The two groups did not significantly differ with respect to sex, age, or years of education (Table 1). All participants with schizophrenia were stabilized outpatients with no change in their treatment during the past month. Most of them were treated with monotherapy (Table 1), and some had additional concomitant medication (mainly hypnotics or anxiolytics). The values for all diffusion parameters and volumes for each tract are presented in Table 2.

TABLE 1. Demographic and clinical characteristics of the study participants

Characteristic	Participants with schizophrenia (N=34)			Healthy individuals (N=69)[a]			p	df
	N	%		N	%			
Male	25	73.5		43	62.3		0.26[b]	1
	Mean	SD	Range	Mean	SD	Range		
Age (years)	37.5	9.1	19.1–59.8	36	9.1	20.9–61.6	0.42[c]	65.8
Education (years)	12.4	2.3	6–17	13	2.5	8–17	0.23[c]	68.7
Illness duration (years)	14.6	8.5	1.4–39.8	NA	—	—	—	
Chlorpromazine equivalents (mg/day)	404.9	310.7	97–1,250	NA	—	—	—	
	N	%		N	%			
Antipsychotic type								
First generation	7	20.6		NA	—	—	—	
Second generation	25	73.5		NA	—	—	—	
Both	1	2.9		NA	—	—	—	
No medication	1	2.9		NA	—	—	—	
	Mean	SD	Range	Mean	SD	Range		
PANSS[d]								
Positive subscale	12.6	5.3	7–24	NA	—	—	—	
Negative subscale	14.6	5.1	8–25	NA	—	—	—	
General subscale	27	6.2	16–45	NA	—	—	—	
Total	54.1	13.2	35–89	NA	—	—	—	

[a] NA=not applicable.
[b] Data were determined using chi-square test, significant at a p value <0.05.
[c] Data were determined using t test, significant at a p value <0.05.
[d] PANSS=Positive and Negative Syndrome Scale. Possible scores range from 30 to 210, with higher scores indicating more severity.

Anatomical Data: SLF I–III, IFOF, and ILF

For the SFLI, a group-by-hemisphere interaction was observed for MD (ANCOVA: F=4.0, df=1, 100, p=0.047); however, Tukey's HSD tests showed no differences.

In the analysis of SLF II, ANCOVAs revealed a significant group-by-hemisphere interaction for all diffusion parameters (FA: F=14.7, df=1, 100, p=0.0002; RD: F=8.8, df=1, 100, p=0.0038; MD: F=4.9, df=1, 100, p=0.030). Healthy individuals presented increased FA and decreased RD/MD in the right hemisphere, compared with participants with schizophrenia (Tukey's HSD tests; FA: F=21.3, df=1, 156, p<0.0001; RD: F=16.3, df=1, 176, p=0.0006; MD: F=11.1, df=1, 179, p=0.0067). Healthy individuals also exhibited increased FA and decreased RD/MD in the right hemisphere, compared with the left hemisphere (Tukey's HSD tests; p<0.0001 for all values; FA: F=65.1, df=1, 104; RD: F=37.2, df=1, 105; MD: F=29.0, df=1, 105) (Figure 2). In participants with schizophrenia, the hemispheres did not differ for any measures.

For the SLF III, we observed a strong tendency for group-by-hemisphere interaction for FA (ANCOVA: F=3.7, df=1, 101, p=0.056). Healthy individuals presented increased FA in the right hemisphere, compared with participants with schizophrenia (Tukey's HSD test: F=20.5, df=1, 177, p<0.0001). Both groups displayed increased FA in the right hemisphere, compared with the left (Tukey's HSD tests; healthy individuals, F=51.8, df=1, 101, p<0.0001; participants with schizophrenia, F=7.2, df=1, 101, p=0.028).

For the IFOF and ILF, ANCOVAs revealed no group-by-hemisphere interaction for any values.

Relationships of Anatomical and Clinical Data

Finally, we computed correlations between anatomical and clinical data and found a significant, negative correlation between FA values for the ILF_L and antipsychotic dosages (p=0.0046, r=−0.48). No other significant correlations emerged.

DISCUSSION

This study was the first to compare structural asymmetry differences in the fiber bundles corresponding to visuospatial attentional abilities in terms of integrity/volume in participants with schizophrenia, compared with healthy individuals. The main findings were reduced integrity in the SLF II (FA, RD, and MD) and the SLF III (FA) in participants with schizophrenia. Participants in both groups exhibited a rightward asymmetry for the SLF III with respect to integrity; by contrast, only healthy individuals presented a rightward asymmetry of the SLF II.

Our results highlight aberrant integrity within the SLF II and the SLF III in participants with schizophrenia, compared with healthy individuals, characterized by neuronal loss (decreased FA) or demyelination of fibers (increased RD and MD). To our knowledge, this study is the first to reveal a difference in integrity between participants with schizophrenia and healthy individuals regarding anatomical organization corresponding to visuospatial abilities. The most striking result of this study is the asymmetry difference between the two groups in the SLF II with respect to integrity. The integrity loss observed in participants with schizophrenia, which was more marked in the SLF II (FA,

TABLE 2. Mean fractional anisotropy (FA), radial diffusivity (RD), and mean diffusivity (MD) values and volume of the fasciculi of the frontoparietal network and the inferior longitudinal fasciculus (ILF) within the right and left hemispheres among participants with schizophrenia compared with healthy individuals[a]

Tract and diffusion parameters	Participants with schizophrenia (N=34)			Healthy individuals (N=69)		
	Mean	SD	Range	Mean	SD	Range
$SLFI_R$						
FA	0.442	0.024	0.40–0.50	0.453	0.030	0.35–0.52
RD	0.577	0.046	0.50–0.72	0.556	0.041	0.49–0.68
MD	0.763	0.042	0.70–0.90	0.744	0.035	0.69–0.86
Vol	3,694.6	1,193.9	1,821–7,101	3,001.4	1,093.7	1,055–6,215
$SLFI_L$						
FA	0.450	0.026	0.40–0.50	0.453	0.030	0.34–0.51
RD	0.569	0.038	0.51–0.70	0.571	0.049	0.51–0.76
MD	0.756	0.045	0.70–0.88	0.760	0.044	0.70–0.93
Vol	3,406.0	1,338.1	1,873–7,915	2,973.7	1,058.9	1,146–6,533
$SLFII_R$						
FA	0.444	0.028	0.38–0.50	0.469	0.023	0.40–0.52
RD	0.554	0.042	0.48–0.65	0.522	0.031	0.46–0.65
MD	0.742	0.037	0.68–0.84	0.718	0.027	0.66–0.81
Vol	4,954.1	1,964.1	2,111–9,319	4,859.8	1,600.4	2,223–10,239
$SLFII_L$						
FA	0.444	0.022	0.38–0.49	0.446	0.026	0.38–0.50
RD	0.557	0.033	0.51–0.63	0.551	0.039	0.50–0.69
MD	0.748	0.031	0.69–0.81	0.741	0.033	0.69–0.86
Vol	4,190.3	1,591.8	2,023–7,618	4,086.0	1,187.9	2,366–7,691
$SLFIII_R$						
FA	0.453	0.021	0.41–0.50	0.478	0.026	0.43–0.54
RD	0.556	0.027	0.49–0.61	0.523	0.032	0.47–0.62
MD	0.751	0.024	0.69–0.79	0.730	0.027	0.68–0.82
Vol	4,619.8	1,175.4	2,933–8,577	4,532.1	1,225.0	2,272–9,095
$SLFIII_L$						
FA	0.440	0.030	0.39–0.51	0.453	0.024	0.39–0.51
RD	0.580	0.053	0.49–0.70	0.558	0.038	0.49–0.70
MD	0.770	0.046	0.70–0.90	0.752	0.032	0.69–0.87
Vol	4,376.3	1,573.1	923–8,211	4,947.3	1,764.2	2,496–9,340
$IFOF_R$						
FA	0.481	0.020	0.45–0.52	0.496	0.022	0.42–0.54
RD	0.569	0.035	0.51–0.66	0.545	0.036	0.49–0.71
MD	0.800	0.034	0.75–0.89	0.784	0.033	0.72–0.93
Vol	4,619.4	804.3	2,619–6,330	4,450.9	804.9	2,643–7,019
$IFOF_L$						
FA	0.493	0.036	0.35–0.55	0.512	0.025	0.45–0.57
RD	0.558	0.042	0.49–0.70	0.535	0.031	0.49–0.62
MD	0.799	0.031	0.75–0.87	0.781	0.026	0.73–0.87
Vol	4,344.4	838.9	1,099–6,078	4,570.2	753.7	3,386–6,754
ILF_R						
FA	0.469	0.030	0.39–0.52	0.483	0.029	0.43–0.55
RD	0.576	0.036	0.51–0.64	0.554	0.034	0.49–0.64
MD	0.798	0.029	0.73–0.85	0.778	0.029	0.71–0.84
Vol	4,497.6	1,597.8	2,361–8,952	4,852.7	1,533.4	2,643–9,652
ILF_L						
FA	0.469	0.027	0.41–0.51	0.480	0.025	0.42–0.54
RD	0.578	0.035	0.51–0.67	0.557	0.022	0.51–0.63
MD	0.804	0.033	0.75–0.88	0.783	0.025	0.74–0.84
Vol	4,671.7	1,399.6	2,639–8,841	4,890.3	1,608.4	2,177–10,327

[a] The MD and RD values were measured in 10^{-3} mm^2/second. IFOF=inferior fronto-occipital fasciculus, L=left hemisphere, R=right hemisphere, SLF I=first branch of the superior longitudinal fasciculus, SLF II=second branch of the superior longitudinal fasciculus, SLF III=third branch of the superior longitudinal fasciculus, Vol=volume in number of voxels.

RD, and MD) and related to both axonal reduction and decreased myelin sheath, might underlie the abnormal asymmetry of this fasciculus in this population. Indeed, previous studies in healthy individuals have shown that a frontoparietal anatomical network, the SLF, supports visuospatial attentional processes, with partial hemispheric lateralization to the right hemisphere (2, 21).

Our results in healthy individuals are in agreement with those of Thiebaut de Schotten et al. (2), who investigated hemispheric specialization of the visuospatial attentional network. They showed that structural lateralization in the SLF with respect to integrity presents a dorsal-ventral gradient characterized by rightward lateralization for the SLF III and SLF II and symmetric organization for the SLF I. Our findings for the participants with schizophrenia suggest a disturbance of this dorsal-ventral gradient that is classically observed in healthy individuals, with a loss of asymmetry in the SLF II. Such changes in this fasciculus could be the source of cognitive deficits in attentional processes.

The differences in anatomical organization observed between the two groups in our study may represent the substrate for differences in visuospatial attentional abilities. The SLF II directly connects the dorsal (SLF III) and ventral (SLF I) streams, which are both especially involved in visual attentional information processing, and appears to modulate between the two. Therefore, SLF II differences may be associated with the visuospatial attentional deficits that accompany schizophrenia (global-local processes [e.g., 13, 39–42]). Further studies are necessary to determine which visuospatial attentional abilities such differences affect.

This study had some limitations. First, regarding participants, the number of patients with schizophrenia was small. We also lacked data on lifestyle factors, such as smoking, for both groups, leaving the potential for cofounding. Moreover, all recruited patients were right-handed and thus represent only a subset of persons with schizophrenia spectrum disorders. A similar study with left-handed participants or a mixture regarding handedness would be interesting. Second, combining structural data with behavioral and functional neuroimaging data might provide finer-grained neuroanatomical information regarding the visuospatial attentional network. Third, the diffusion-weighted image sequence was limited to 21 gradient directions and to a b-value of 1,000, which does not completely overcome issues of crossing and branching fibers. For this reason, we did not test axial or parallel diffusivity (i.e., parallel diffusivity, the diffusion of water along the direction of the principal diffusion), because it lacks sensitivity for regions with branching and crossing white matter fibers (38), such as the intrahemispheric tracts included here. Fourth, we carried out our analyses with SPM5 rather than SPM12. We made this choice because data for our sample were previously acquired and preprocessed for other studies using SPM5 (43). Nevertheless, we conducted a crucial quality control on the ten tracts of the 103 participants. In addition, SPM was used only to transfer tracts/diffusion maps into the MNI common space and not for extracting quantitative data. Finally, we did not directly investigate the visuospatial attentional network because the white matter fasciculi connecting its regions do not really constitute a network; thus our results should be interpreted with caution. Despite these limitations, this study is the first to describe the structural organization of fasciculi underlying visuospatial attentional abilities in schizophrenia.

FIGURE 2. Differences in integrity between participants with schizophrenia and healthy individuals in branch II of the superior longitudinal fasciculus[a]

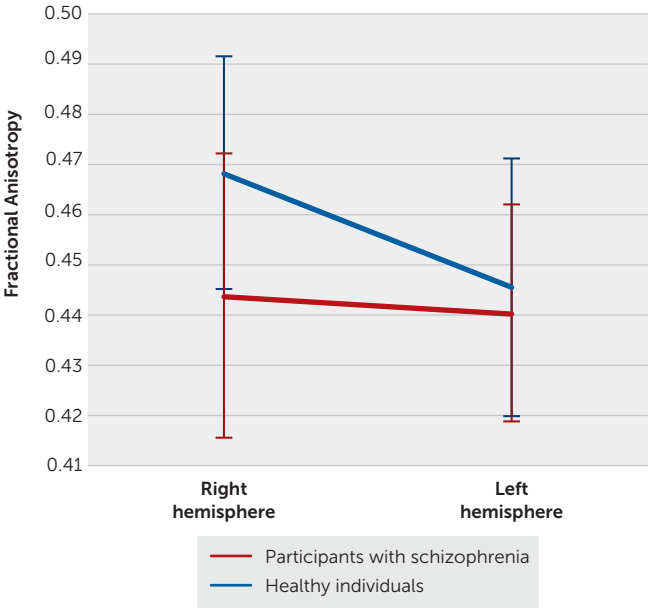

[a] Healthy individuals displayed a rightward asymmetry ($p<0.0001$), in which there was greater integrity (increased fractional anisotropy), compared with participants with schizophrenia ($p<0.0001$).

CONCLUSIONS

Our findings revealed a specific disruption of structural connectivity (loss of integrity) in the SLF II and abnormal anatomical asymmetry (loss of asymmetry) of this fasciculus between the two hemispheres in participants with schizophrenia. These abnormalities could be one substrate of attentional deficits and alterations that underlie visuospatial disabilities in people with schizophrenia. The results provide new insight into the neuroanatomical basis of the atypical visuospatial attentional network in schizophrenia and offer new understanding of how people with schizophrenia perceive and process their visual world.

AUTHOR AND ARTICLE INFORMATION

The Department of Psychiatry, Université de Caen Normandie, Caen, France (Leroux, Dollfus); Université de Paris, LaPsyDÉ, UMR 8240, CNRS, Paris (Poirel); Institut Universitaire de France, Paris (Poirel); Service de Psychiatrie Adulte, Centre Hospitalier Universitaire de Caen, Caen, France (Dollfus); and the Department of Psychiatry, UFR de Médecine, Université de Caen Normandie, Caen, France (Dollfus).

Send correspondence to Dr. Leroux (eleroux@cyceron.fr).

Supported by the Regional French Health Ministry's Programme Hospitalier de Recherche Clinique 2005 (grant CHU 05-097).

The authors thank Annick Razafimandimby, Ph.D., Frederic Briend, Ph.D., and Vincent Marzloff, Ph.D., for their technical assistance and Perrine Brazo, Ph.D., for her clinical contribution.

The funding sources were not involved in the study design; data collection, analysis, or interpretation; writing of the manuscript; or the decision to submit the manuscript for publication.

The authors report no financial relationships with commercial interests.

Received April 26, 2019; revision received September 12, 2019; accepted October 28, 2019; published online Jan. 17, 2020.

REFERENCES

1. Lunven M, Bartolomeo P: Attention and spatial cognition: neural and anatomical substrates of visual neglect. Ann Phys Rehabil Med 2017; 60:124–129
2. Thiebaut de Schotten M, Dell'Acqua F, Forkel SJ, et al: A lateralized brain network for visuospatial attention. Nat Neurosci 2011; 14:1245–1246
3. Gazzaniga MS: Cerebral specialization and interhemispheric communication: does the corpus callosum enable the human condition? Brain 2000; 123:1293–1326
4. Knecht S, Dräger B, Deppe M, et al: Handedness and hemispheric language dominance in healthy humans. Brain 2000; 123: 2512–2518
5. Knecht S, Deppe M, Dräger B, et al: Language lateralization in healthy right-handers. Brain 2000; 123:74–81
6. Alary M, Delcroix N, Leroux E, et al: Functional hemispheric lateralization for language in patients with schizophrenia. Schizophr Res 2013; 149:42–47
7. Dollfus S, Razafimandimby A, Delamillieure P, et al: Atypical hemispheric specialization for language in right-handed schizophrenia patients. Biol Psychiatry 2005; 57:1020–1028
8. Leroux E, Delcroix N, Dollfus S: Left fronto-temporal dysconnectivity within the language network in schizophrenia: an fMRI and DTI study. Psychiatry Res 2014; 223:261–267
9. Leroux E, Delcroix N, Dollfus S: Left-hemisphere lateralization for language and interhemispheric fiber tracking in patients with schizophrenia. Schizophr Res 2015; 165:30–37
10. Catani M, Craig MC, Forkel SJ, et al: Altered integrity of perisylvian language pathways in schizophrenia: relationship to auditory hallucinations. Biol Psychiatry 2011; 70: 1143–1150
11. Cavelti M, Winkelbeiner S, Federspiel A, et al: Formal thought disorder is related to aberrations in language-related white matter tracts in patients with schizophrenia. Psychiatry Res Neuroimaging 2018; 279:40–50
12. Viher PV, Stegmayer K, Giezendanner S, et al: White matter correlates of the disorganized speech dimension in schizophrenia. Eur Arch Psychiatry Clin Neurosci 2018; 268:99–104
13. Poirel N, Brazo P, Turbelin MR, et al: Meaningfulness and global-local processing in schizophrenia. Neuropsychologia 2010; 48: 3062–3068
14. Uhlhaas PJ, Mishara AL: Perceptual anomalies in schizophrenia: integrating phenomenology and cognitive neuroscience. Schizophr Bull 2007; 33:142–156
15. Hahn B, Robinson BM, Harvey AN, et al: Visuospatial attention in schizophrenia: deficits in broad monitoring. J Abnorm Psychol 2012; 121:119–128
16. Mesulam MM: Large-scale neurocognitive networks and distributed processing for attention, language, and memory. Ann Neurol 1990; 28:597–613
17. Corbetta M, Shulman GL: Control of goal-directed and stimulus-driven attention in the brain. Nat Rev Neurosci 2002; 3:201–215
18. Thiebaut de Schotten M, Dell'Acqua F, Valabregue R, et al: Monkey to human comparative anatomy of the frontal lobe association tracts. Cortex 2012; 48:82–96
19. Doniger GM, Foxe JJ, Murray MM, et al: Impaired visual object recognition and dorsal/ventral stream interaction in schizophrenia. Arch Gen Psychiatry 2002; 59:1011–1020
20. Stiles J, Akshoomoff N, Haist F: The development of visuospatial processing: neural circuit development and function in the healthy and diseased brain; in Comprehensive Developmental Neuroscience: Neural Circuit Development and Function in the Brain, vol 3. Edited by Rubenstein JLR, Rakic P. Amsterdam, Elsevier, 2013
21. Chechlacz M, Gillebert CR, Vangkilde SA, et al: Structural variability within frontoparietal networks and individual differences in attentional functions: an approach using the theory of visual attention. J Neurosci 2015; 35:10647–10658
22. Ortibus E, Verhoeven J, Sunaert S, et al: Integrity of the inferior longitudinal fasciculus and impaired object recognition in children: a diffusion tensor imaging study. Dev Med Child Neurol 2012; 54:38–43
23. Philippi CL, Mehta S, Grabowski T, et al: Damage to association fiber tracts impairs recognition of the facial expression of emotion. J Neurosci 2009; 29:15089–15099
24. Urbanski M, Thiebaut de Schotten M, Rodrigo S, et al: Brain networks of spatial awareness: evidence from diffusion tensor imaging tractography. J Neurol Neurosurg Psychiatry 2008; 79: 598–601
25. Bauer CM, Heidary G, Koo BB, et al: Abnormal white matter tractography of visual pathways detected by high-angular-resolution diffusion imaging (HARDI) corresponds to visual dysfunction in cortical/cerebral visual impairment. J AAPOS 2014; 18: 398–401
26. Beaulieu C: The basis of anisotropic water diffusion in the nervous system: a technical review. NMR Biomed 2002; 15:435–455
27. Song JW, Mitchell PD, Kolasinski J, et al: Asymmetry of white matter pathways in developing human brains. Cereb Cortex 2015; 25:2883–2893
28. Thiebaut de Schotten M, Ffytche DH, Bizzi A, et al: Atlasing location, asymmetry and inter-subject variability of white matter tracts in the human brain with MR diffusion tractography. Neuroimage 2011; 54:49–59
29. Kay SR, Fiszbein A, Opler LA: The Positive and Negative Syndrome Scale (PANSS) for schizophrenia. Schizophr Bull 1987; 13: 261–276
30. Leroux E, Delcroix N, Alary M, et al: Functional and white matter abnormalities in the language network in patients with schizophrenia: a combined study with diffusion tensor imaging and functional magnetic resonance imaging. Schizophr Res 2013; 150: 93–100
31. Tzourio-Mazoyer N, Landeau B, Papathanassiou D, et al: Automated anatomical labeling of activations in SPM using a macroscopic anatomical parcellation of the MNI MRI single-subject brain. Neuroimage 2002; 15:273–289
32. Mori S, van Zijl P: Human white matter atlas. Am J Psychiatry 2007; 164:1005
33. Smith SM, Jenkinson M, Woolrich MW, et al: Advances in functional and structural MR image analysis and implementation as FSL. Neuroimage 2004; 23(suppl 1):S208–S219
34. Behrens TE, Johansen-Berg H, Woolrich MW, et al: Non-invasive mapping of connections between human thalamus and cortex using diffusion imaging. Nat Neurosci 2003; 6:750–757
35. Hecht EE, Gutman DA, Bradley BA, et al: Virtual dissection and comparative connectivity of the superior longitudinal fasciculus in chimpanzees and humans. Neuroimage 2015; 108:124–137
36. Catani M, Thiebaut de Schotten M: A diffusion tensor imaging tractography atlas for virtual in vivo dissections. Cortex 2008; 44: 1105–1132

37. Catani M, Jones DK, Donato R, et al: Occipito-temporal connections in the human brain. Brain 2003; 126:2093–2107
38. Alexander AL, Lee JE, Lazar M, et al: Diffusion tensor imaging of the brain. Neurotherapeutics 2007; 4:316–329
39. Chen Y, Nakayama K, Levy D, et al: Processing of global, but not local, motion direction is deficient in schizophrenia. Schizophr Res 2003; 61:215–227
40. Johnson SC, Lowery N, Kohler C, et al: Global-local visual processing in schizophrenia: evidence for an early visual processing deficit. Biol Psychiatry 2005; 58:937–946
41. Coleman MJ, Cestnick L, Krastoshevsky O, et al: Schizophrenia patients show deficits in shifts of attention to different levels of global-local stimuli: evidence for magnocellular dysfunction. Schizophr Bull 2009; 35:1108–1116
42. Landgraf S, Amado I, Purkhart R, et al: Visuo-spatial cognition in schizophrenia: confirmation of a preference for local information processing. Schizophr Res 2011; 127:163–170
43. Madigand J, Tréhout M, Delcroix N, et al: Corpus callosum microstructural and macrostructural abnormalities in schizophrenia according to the stage of disease. Psychiatry Res Neuroimaging 2019; 291:63–70